PUSH-OVER NON LINEAR ANALYSIS OF INFILLED FRAMES: REALISTIC F E MODELS OF PANELS AND CONTACT

Frederick Ellul[1] and Dina D'Ayala[2]

[1] *Associate, Ramboll WhitbyBird , 60 Newman Street, London,W1T3DA, UK*
[2] *Senior Lecturer, Dept. of Architecture and Civil Engineering, University of Bath, Bath,BA2 7AY, UK*
Email: frederick.ellul@rambollwhitbybird.com, D.F.D'Ayala@bath.ac.uk

ABSTRACT :

A finite element based modelling technique that enables the representation of the masonry infills in an analytical environment suitable for use in the assessment of low engineered masonry infilled reinforced concrete frame (LE-MIRCF) buildings has been developed. The mezo-modelling approach adopted for the masonry infills was implemented in a non-linear finite element environment. Fibre elements are used to represent the reinforced concrete members and a spring element for the interface between these and the masonry. The approach has been used to explore the effects of imposing different masonry infill distributions throughout a typical internal frame of a five storey LE-MIRCF structure which was analysed in the inelastic range, and its performance assessed. It is shown that the provision of masonry infills is not always detrimental nor always beneficial, but depends on the particular infill configuration, thereby justifying the approach used.

KEYWORDS: Masonry infills, reinforced concrete, push-over analysis

1. INTRODUCTION

During ongoing research at the University of Bath on the behaviour of LE-MIRCF constructions, it became apparent that analytical techniques as found in the literature for these constructions are not entirely suitable for their seismic assessment. This principally stems from the widespread use of the inclined strut approach and its variants to represent masonry infills in numerical models. In fact the inability of the latter technique to predict suitable estimates of the actual action effects within the reinforced concrete members must be considered as a serious drawback for its use in assessing the performance of LE-MIRCF structures subjected to significant ground motions. This is confirmed by post earthquake observations which show that significant damage in these buildings invariably take the form of local failure in the reinforced concrete columns, induced by the interaction effects with the masonry infills. Thus, though the infills heavily influence the structural behaviour of LE-MIRCF constructions, it is not their own detailed response which is of major concern, but rather the ability of a technique to simulate the geometric and physical representation of an entire structure.

A mezo-modelling technique using a continuum model for the analysis of masonry infills has therefore been formulated, wherein each masonry finite element consists of a four noded three dimensional isoparametric membrane element, with no rotational stiffness or stiffness normal to its plane, (Ellul, 2006). This then represents several bricks and mortar joints, wherein the material can be regarded as a homogenous one. Two failure modes were implemented, one associated with the tensile strength of the material and the other in terms of its compressive strength. The latter behaviour was represented by applying an elasto-plastic approach with an idealised stress-strain relationship, where once a certain level of stress has been reached within the material an irreversible straining ensues for a further increase in stress. This perfectly plastic response is assumed until the crushing surface is encountered when the material is assumed to lose all its characteristics of strength and rigidity. On the other hand the stress-strain relationship of masonry in tension was modelled as a linear-elastic fracture model including a tension cut-off criterion. An average representation for cracked masonry using a smeared cracked approach was implemented, which ensured that the influence of the cracked masonry zones on the overall structural behaviour, especially in respect to the induced action effects within the

frame elements was also modelled.

During each load increment the element algorithm implemented works within the overall solution procedure. Whereby at the beginning of the n^{th} load increment the displacements a^{n-1} and the stresses σ^{n-1} are known, as well as the unbalanced forces u^{n-1} from the previous load increment. The incremental nodal forces are calculated according to, $u_o^{\,n} = u^{n-1} + \Delta f^{\,n}$. Where u^{n-1} are the residuals existing at the end of the previous load increment and Δf^n is the n^{th} load increment. Subsequently, the iterative process is performed with the following steps for a generic iteration i:

Step 1 The stiffness matrix K is updated

Step 2 The incremental displacements Δa_i are evaluated using the equilibrium equations, $\Delta a_i = -[K]^{-1} u_{i-1}$ Where u_{i-1} are the unbalanced nodal forces resulting from the previous iteration. The total displacement vector a_i is then updated, $a_i = a_{i-1} + \Delta a_i$

Step 3 The incremental strains $\Delta\varepsilon_i$ and the total strains ε_i are evaluated, $\Delta\varepsilon_i = B_o \Delta a_i$ and $\varepsilon_i = B_o a_i$ Where B_o is the compatibility matrix, as geometrical nonlinear behaviour is not considered.

Step 4 The incremental stresses $\Delta\sigma_i$ and the total stresses σ_i are calculated, $\Delta\sigma_i = D\Delta\varepsilon_i$ and $\sigma_i = \sigma_{i-1} + \Delta\sigma_i$ Where D is the elasticity matrix taken as either the elastic matrix of uncracked masonry or the corresponding matrix of cracked masonry

Step 5 The stresses are corrected according to the material constitutive equations: (a) Using the total stresses σ_i, the maximum principal stress σ_1, acting in the structural plane, is calculated. (b) If $\sigma_1 > f'_t$ or if the masonry is already cracked, the stresses are updated according to the tensile modelling. (c) Using σ_i or the stresses updated in the previous step, the effective stress, σ_e is calculated according to the yield function. (d) If σ_e is greater than the initial yield stress or if it has already yielded, the stresses are corrected according to the elasto-plastic behaviour.

Step 6 The equivalent internal forces are evaluated.

Step 7 The out of balance forces are calculated.

Step 8 The convergence process is checked. If convergence has been achieved, then proceed to the next load increment. On the other hand if the convergence criterion has not been satisfied restart the iterative cycle from step 1.

The masonry element is combined with an overall modelling strategy for simulating LE-MIRCF constructions, and implemented in a numerical environment widely used in the field of earthquake engineering, DRAIN-3DX, (Prakash et al. 1994). Reinforced concrete members were modelled using a distributed plasticity type fibre element as found within DRAIN-3DX (Powell and Campbell, 1994). The boundary between the reinforced concrete frame elements and the masonry infill panel is modelled by using interface elements. The behaviour at this location is one of the most important aspects in infilled frame modelling, as the frame may separate from the panel. Therefore, the inclusion of interface elements allows for the ability to simulate the separation between the frame members and the masonry infill, once the initial bond provided by the mortar is overcome. Therefore, element type 1, as found in DRAIN-3DX (Powell and Campbell, 1994), was used for the interface elements which only transmits axial load and has the ability to yield both in tension and compression. The stiffness of the element is assumed to be infinitely rigid when there is no gap, and reduces to zero once separation occurs.

An assessment methodology was finally formulated which hinges on the ability of the modelling technique to predict sufficiently accurate estimates of the action effects within the reinforced concrete members, especially to predict shear failures in the members taking into account the interaction of all the action effects in determining their shear capacity. Thus, allowing for a better overall estimate of the seismic capacity of LE-MIRCF constructions. This technique was then used to investigate geometrical irregularity caused by different infill configurations throughout a typical frame structure.

2. THE STRUCTURAL FRAME

In order to concentrate on the effects induced from the irregularity caused by the infill distribution the prototype bare frame structure is regular throughout its height and is an internal frame of a three dimensional building, as shown in Figure 1, with the orientation of the columns defined by the column's major axis and therefore in the stronger direction. The frame is five storeys high, with a storey height of 3.15 metres. The bay lengths are 5m-3.5m-5m in the main direction. The slab thickness is 150 mm and is reinforced with 8 mm diameter bars at 200 mm centres, both ways. Column dimensions, are 600 x 300 mm, with reinforcement that comprises 18 mm diameter bars in the longitudinal direction and 8 mm diameter stirrups at 250 mm centres in the transverse directions with the column sections remaining constant throughout the building height, both in size and steel amount. Both main and secondary beams include the slab thickness and 500 mm high downstands, with a width of 300mm. Beam reinforcement at the top is constituted of four 18 mm diameter bars, whilst the bottom reinforcement consists of two 18 mm diameter bars over the interior columns which increase to three at mid-span. Furthermore, beam transverse reinforcement is composed of 8 mm diameter stirrups at 200 mm centres and do not continue in the beam-column joints.

The concrete strength was assumed to have a mean compressive cylinder strength of 16 MPa, whilst the reinforcement was mild steel and presumed to be characterised by an average yield strength of 250 MPa, with a corresponding mean ultimate tensile strength of 350 MPa. As regards the masonry infills, these were assumed as single leaf and constructed of hollow clay bricks 130 mm thick, laid in a cement-lime mortar. The masonry infill considered is representative of a weak masonry having a compressive strength of 1.0 MPa over the gross area. The geometry and material characteristic, together with the fact that the infill is in direct contract to the frame reflect common construction practice in Europe before the second generation seismic codes and also currently in many developing countries where infill frames are not engineered to resist earthquakes.

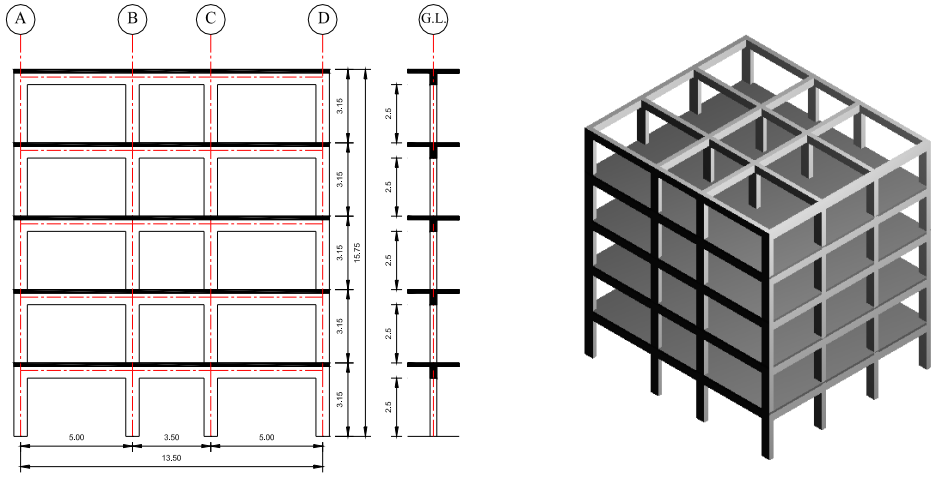

Figure 1 The prototype structure (a) Left - Section of internal frame (b) Right - Three dimensional view of the reinforced concrete bare frame structure.

3. THE INFLUENCE OF DIFFERENT MASORY INFILL DISTRIBUTION

The effect of infill distribution on LE-MIRCF constructions was then explored by classifying the various geometrical possibilities into three main categories. The first group marked A, specifically dealt with the consequences of omitting an entire bay of infills throughout the height of the structure, thus representing a relatively uniform distribution of stiffness throughout the height of the frame. On the other hand, group B examined the effects of omitting infills from certain floors only, such as with the infamous soft storey

configuration, whilst the third set investigated the influence of different opening configurations on the structural performance.

The load deformation responses of the numerical specimens were followed through to failure by means of the capacity curve. The latter was established using nonlinear static pushover analysis, wherein the loading profile used was a triangular one, commensurate to the dominant first mode distribution of the seismic loads. Gravity loads accounted for during the analysis included the selfweight of the reinforced concrete members, a finishes surcharge of 1.0 kN/m^2 and a live loading of 2.0 kN/m^2, only 30% of which was considered for the seismic load combination. Moreover, all infill partitions were assumed to be located on the beams. Their weight was accounted for by assuming a uniform beam load of 3.6 kN/m per metre run of the wall, which was included in the model by means of an axial load on the beam column joint imparted from the beam reaction.

3.1. Limit State Criteria

In order to assess the seismic performance of each structure throughout the nonlinear analysis, performance points or limit states were defined both on a local member level and also on the entire structure. Such an approach enables damage assessment and failure prediction by monitoring and comparing the demands imposed by the lateral load and the corresponding capacities of the individual members, together with the deformation capacity of the whole structure (FIB, 2003; Penelis and Kappos, 1997). On violation of any single local criterion, overall structural collapse is not expected and only the implication of a probable level of damage is had. Hence, the performance criteria adopted inevitably results in a conservative prediction of the ultimate deformation limit of the structure, since the incipient point of collapse is fraught with uncertainties and therefore not of palpable interest. The following performance points were evaluated at each step of the analysis commensurate with the requirements of many modern assessment guidelines (FIB, 2003; FEMA 356; NZ, 1996):

(a) Local criterion: Attainment of maximum member curvature by exceedance of ultimate compressive strain in concrete.
(b) Local criterion: Exceeding the shear force capacity of the members.
(c) Local criterion: Beam-column joint shear capacity, according to the method found in the NZ (1996)
(d) Global criterion: Relative interstorey drifts.

All the local performance criteria were monitored for each individual member. However, it was assumed that the performance point representing collapse and hence ultimate displacement capacity for the structure was identified only by the occurrence of only two of the above cases. These included the satisfaction of the global criterion or the instance when the concrete strain in a column attained a value of 0.005, signifying concrete crushing as per FIB (2003) and FEMA 356. The latter was included since such an event might imply an inter-storey collapse, especially in the frame considered, where each storey is supported by only four columns. On the other hand, shear failures in the columns, though recorded, were not considered as being as detrimental, since many instances of columns having wide distinct shear cracks are reported in post event records (Ellul, 2006). Beam failures of any type were also allowed, on the assumption that a small number of them would not jeopardise the gravity load bearing capacity of the structure, due to the expected redistribution of loads.

As regards the global criterion, the maximum relative inter-storey drift occurring in the structure has long been recognised as an indicator for seismic assessment. However, agreement on the appropriate value adopted for realistic representation of the various limit states is another matter all together, as codes of practice generally define values corresponding to the serviceability limit state. The definition of the ultimate limit state drift is then usually based on engineering judgement, following post-earthquake field observations. Therefore, a limit of 1.25% was adopted in this case, based on the recommendations of Repapis et al. (2006) for existing reinforced concrete frames with limited ductility, in order to account for any significant P-Delta effects which would set in beyond that point.

4. COMPARISON OF STRUCTURAL BEHAVIOUR

The relative performance of each configuration is reviewed by means of the capacity curves for each analysis series. In these figures, for a clearer presentation, the local performance points are only shown when attained in the column members. However, apart from predicted joint damage failure in the bare frames and beam yielding in all the structures, no other damage was predicted apart from that shown. As regards the effects of the infill distribution on the performance of the assemblage, each case was plotted together with the corresponding capacity curves for the bare frame case and the fully infilled frame case, which bound the behaviour of each partially infilled structure, thus allowing easier comparison.

On comparing the behaviour of the fully infilled frames, case A1, against the behaviour of the bare frame, it was seen that the introduction of the infills resulted in a lower deformation capacity of around 10%, though the overall lateral strength capacity was increased by over 30%. Furthermore, the gain in initial stiffness caused by the presence of the infills was of 2.5 times. The effect of omitting the infills entirely from the vertical bays was studied in the analyses series A2 to A4. The deformation capacity of these new structures was at least as good as for the fully infilled frame, in two out of three instances marginally better, whilst the lateral load capacity decreased due to the lower area of infills present, as shown in Figure 2. In general therefore for this particular structural configuration, the omission of an entire bay of infills throughout its height did not prove detrimental to the structural performance. As regards to predicted shear failures in the columns, specimen A3 is predicted to suffer shear column failure at the top of the ground storey columns, close to the spalling performance point. Hence, if the shear performance point was taken as the displacement limit, the total decrease in predicted displacement capacity would be no less than 15%, but then just before the concrete crushing strain is attained, which is understandable given the significant column depth in this case. The first yielding, spalling and crushing of the columns generally occurred at the same deformation level as for the fully infilled case, and slightly earlier than for the bare frame case.

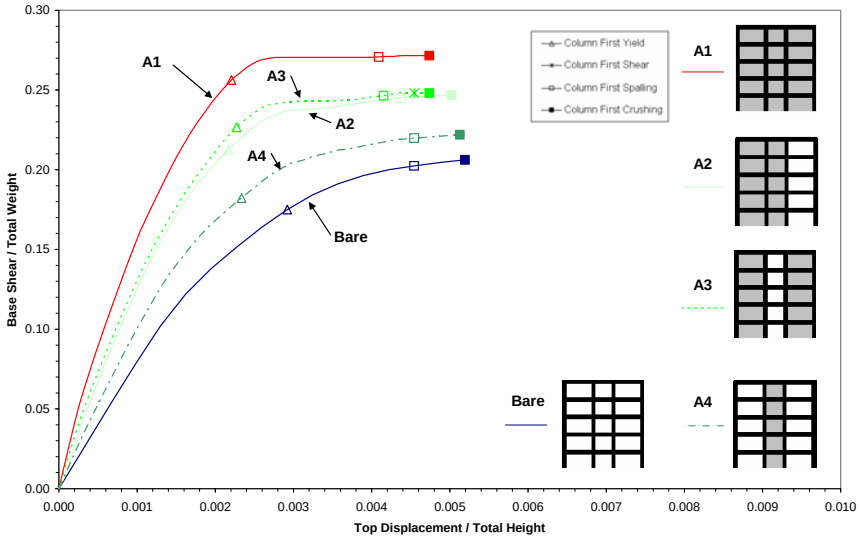

Figure 2 Capacity curves – A series.

On the other hand significant differences in behaviour were noticed for the structures in the B series, which set out to identify behaviour due to significant change in stiffness between adjacent storeys. As expected the soft ground storey structure represented by case B1, resulted in a much reduced displacement capacity with a decrease of no less than 35%. Interestingly however, the configuration did not result in the lowest ultimate load capacity gain, which was attained by series A4. Furthermore, from Figure 3 which depicts the capacity curves, it was also noticed that configuration B1 attained an ultimate displacement capacity of 0.3% drift. As regards configuration B2 the performance was very similar to that of the fully infilled frame, both in terms of ultimate lateral load capacity and ultimate deformation capacity as well as the inter-storey drift. The infill at the top storey therefore did not provide just capacity improvement but a slight stiffness increase. Indeed, from the

analysis performed it was evident that the higher mode effects which would impose a higher demand on the upper floor were not reproduced in this case, and the structure remained relatively unscathed at this location. This is contrary to the evidence from the field (Ellul, 2006), which suggests an increased vulnerability for the upper floor, with collapse at this level being registered prior to that in the lower floors. It is only from Figure 4, which details the inter-story drifts at predicted collapse, that an increased demand on the top floor was observed. However, for this assemblage the suitability of using the conventional nonlinear pushover technique with triangular distribution is severely tested and the possibility of using an adaptive pushover scheme should be investigated further. Such a conclusion is in agreement with those derived by other researchers, (Dolce et al., 2005; Elnashai, 2002). For specimen B3 a reduced overall capacity was registered.

The possible formation of a weak storey by omitting just a single bay of the infills at ground floor level was represented by series B4. This proved to be detrimental so much so that the configuration had a decreased deformation capacity of over 20%. Consequently, when compared to the soft storey structure of series B1 it performed better, by as much as 20% for the ultimate deformation capacity, accompanied by an increased ultimate load capacity and initial stiffness. This particular configuration clearly illustrates that even a small change in the masonry infill distribution can prove highly detrimental to the overall lateral structural behaviour, hence the importance of applying a rational modelling technique in assessing the latter's performance. Overall, the change in stiffness induced by the different infill configurations proved to be very damaging for the B test series except for the B2 case. Nevertheless, these configurations did not give rise to premature shear failures, as concrete crushing proved to be the more damaging mechanism in all cases, even those with a soft storey.

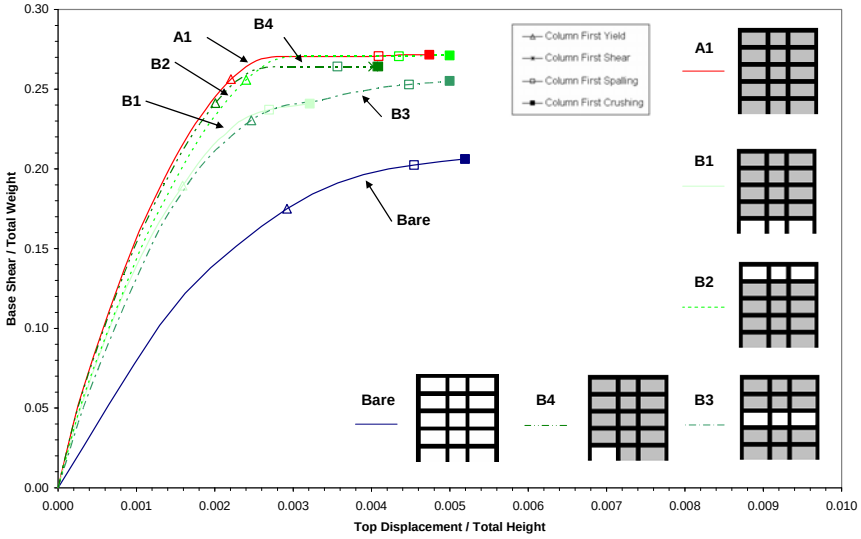

Figure 3 Capacity curves – B series.

The effect of different openings in the masonry infills was studied in the C analysis series, as shown in Figure 5. Case C1 considered centrally positioned windows in each panel with a void to infill ratio of around 0.13, while C2 has similarly positioned doors with a void ratio of 0.19. In both these cases, minimal changes from the behaviour of the fully infilled frame were noticed, especially in terms of deformation capacity. However, where irregular openings were included such as in cases C3, C4 and C5 the performance of the structure was adversely affected with all three configurations registering significant decrease in the ultimate deformation capacity as compared to the fully infilled frame case. Cases C3 and C4 were intended to represent the rather common occurrence of short or captive columns, and two different scenarios were studied. The first variant was for configuration C3, where the openings did not continue up to the column face, whilst the second, case C4, had a continuous opening right across the infill up to the column face. This slight difference in geometry resulted in an increased vulnerability for the latter case, with a difference in deformation capacity of over 10% between the two, and attained at lower ultimate lateral loads.

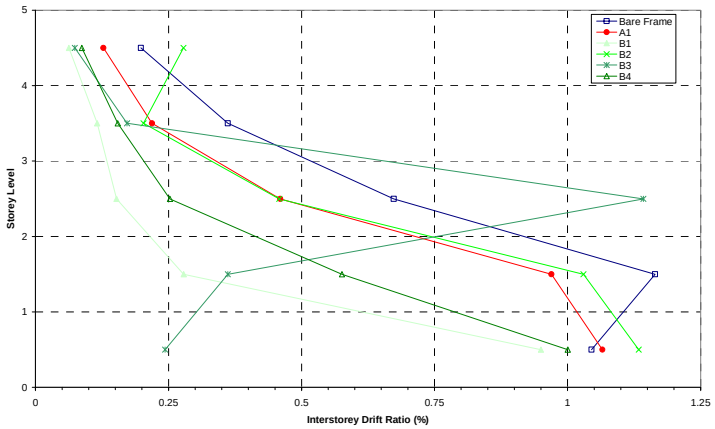

Figure 4 Inter-storey drifts at the ultimate displacement for the B series.

The difference in behaviour between the two is further appreciated by referring to Figure 6 depicting the inter-storey drifts. In fact it is seen that the mechanism at failure predicted for assemblage C3 is similar to that for the fully infilled frame A1, however that of configuration C4 resembles that of the soft storey assemblage B1. Indeed, comparison of these analysis cases demonstrates the importance of accurately representing the geometrical characteristics of each construction, whilst they attest to the strength of the proposed modelling methodology. No shear failure before crushing of the concrete was reached, which at first glance appears to be inconsistent with the observations in the field. However, on closer inspection this was attributed to the fact that the columns were oriented in the strong direction with its increased shear strength capacity of its columns, due to twice the effective depth being available when compared to the minor axis. Indeed, further analysis with the column oriented about the weak axis proved this to be the case. Finally, analysis case C5 investigated the effect of having door openings only at ground floor level, thereby simulating the instigation of a possible weak ground storey mechanism, as corroborated by the predicted inter-storey drifts in Figure 6. In this case this configuration also proved to be detrimental to the overall performance of the structure.

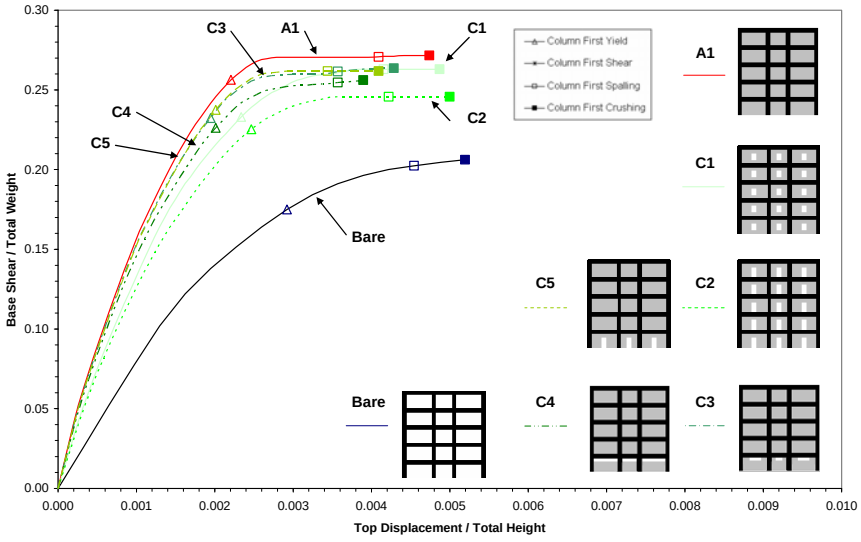

Figure 5 Capacity curves – C series.

The C test series also attests to the versatility of the modelling methodology applied. Indeed, the configurations studied could not have been confidently analysed using the inclined strut approaches, which is cumbersome and irrational when used for such configurations. Conversely, the modelling technique employed allowed for even minor changes in the geometric characteristics of the openings, such as was the case between specimens C3 and C4, where appreciable differences in behaviour where noticed between the two.

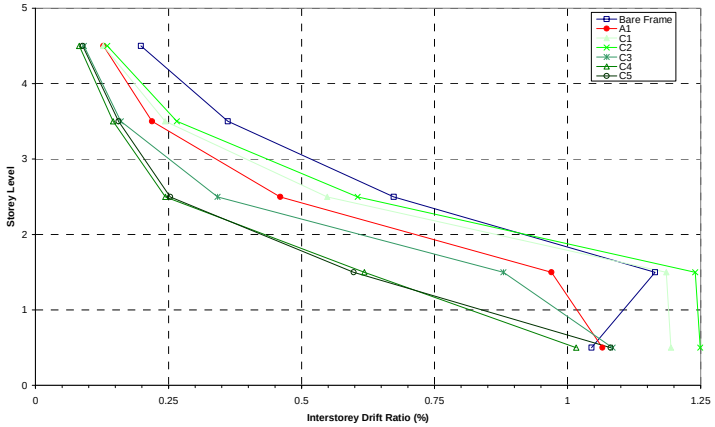

Figure 6 Inter-storey drifts at the ultimate displacement for the C series.

5. CONCLUSION

The parametric analyses confirmed the significant influence of the masonry infill distribution on the performance of the structure, with certain configurations proving highly detrimental and possessing unique characteristics. This corroborates perceptions gathered from field observations, that certain infill distributions actually precipitate overall structural failure merely by their layout or geometrical features, such as the position of doors and windows adjacent to columns. Nevertheless, it has also been shown that the fully infilled frame configuration undoubtedly outperformed the bare frame structure and had improved survivability. Conversely, the soft storey configuration proved highly unfavourable. However, the delicate balance between improvement and degradation of the response is had by reference to series B4 and C4, where slight adjustments to the infills eliminated any advantage from the infill presence altogether. It has therefore been shown that the provision of masonry infills is not always detrimental nor always beneficial, but rather depends on the particular configuration and the way this alters the buildings stiffness locally. The importance of using a numerical model such as the one presented for the seismic assessment of LE-MIRCF constructions has also been revealed, since the accurate representation of the actual masonry infill geometrical characteristics can actually determine the entire outcome of the assessment procedure.

REFERENCES

Dolce, M., Kappos, A. J., Masi, A., Penelis, G. and Vona, M. (2005). Vulnerability assessment and earthquake damage scenarios of the building stock of Potenza (Southern Italy) using Italian and Greek methodologies. *Engineering Structures*, **28**, pp 357-371.

Ellul, F. (2006). Static nonlinear finite element analysis of low engineered masonry infilled reinforced concrete frames for seismic assessment, PhD Thesis, Dept. of Architecture & Civil Engineering, University of Bath, UK.

Elnashai, A. S. (2002). Do we really need inelastic dynamic analysis. *Journal of Earthquake Engineering*, **6**, **Special Issue 1**, pp 123-130.

FEMA 356. Prestandard and commentary for the seismic rehabilitation of buildings. (ASCE 2000) Prepared by the American Society of Civil Engineers for the Federal Emergency Management Agency, Washington, D.C.

FIB (2003). Seismic assessment and retrofit of reinforced concrete buildings. State-of-the-art report, International Federation for Structural Concrete.

NZ (1996). The assessment and improvement of the structural performance of earthquake risk buildings. Draft for general release. For the Building Industry Authority by the New Zealand National Society for Earthquake Engineering.

Prakash, V., Powell, G .H. and Campbell, S. (1994) *Drain-3DX Base program description and user guide.* Version 1.10, Department of Civil Engineering, University of California, Berkeley, California.

Penelis, G. G. and Kappos, A. J. (1997). Earthquake-resistant concrete structures. E & FN Spon., London.

Repapis, C., Vintzileou, E and Zeris, C. (2006). Evaluation of the seismic performance of existing RC buildings: I. suggested methodology. *Journal of Earthquake Engineering*, **Vol. 10**, **No. 2**, pp 265-287.